Cement and Concrete Research 39 (2009) 754–762

Contents lists available at ScienceDirect

Cement and Concrete Research

journal homepage: http://ees.elsevier.com/CEMCON/default.asp

A multiscale model for modulus of elasticity of concrete at high temperatures

Jaesung Lee [a], Yunping Xi [b,*], Kaspar Willam [b], Younghan Jung [c]

[a] Hannam University, 133 Ojung, Daeduk, Daejeon, 306-791, South Korea
[b] Department of Civil Engineering, University of Colorado, Boulder, CO, 80309, USA
[c] LCCKOREA Co. Ltd., 800 Doan, Seo-Gu, Daejeon, 302-318, South Korea

ARTICLE INFO

Article history:
Received 19 April 2007
Accepted 25 May 2009

Keywords:
Composite mechanics
Modulus of elasticity
High temperature
Concrete

ABSTRACT

In this paper, the thermal degradation of modulus of elasticity of concrete is modeled by composite mechanics at three scales of observation: (a) at the level of concrete, (b) at the level of mortar, and (c) the cement paste level. At the latter, the change of volume fractions of the constituents are evaluated based on phase transformations which take place in different temperature ranges. Stoichiometric models are used to determine the volume changes of the constituents. At the mortar and concrete levels, the temperature dependence of fine and coarse aggregates is considered based on available test data. The multiscale chemo-mechanical model can be used to predict the temperature dependence and thermal degradation of the elastic concrete modulus. The model predictions are compared with test data in the literature as well as in-house test data.

1. Introduction

Stiffness of concrete decreases with increasing temperatures. The degradation results mainly from two mechanisms. The first one is related to the temperature sensitivity of the mechanical properties of the constituents in concrete. Stiffness of each constituent decreases with increasing temperature, which leads to the degradation of the composite. The second mechanism is related to phase transformations of constituents at different temperatures. The initial constituents of concrete transform to other phases due to elevated temperature. The new phases tend to have lower stiffness than the original phases. Therefore, the degradation of concrete under high temperatures must be studied from both mechanical and chemical points of view. Since the size of the concrete constituents range from centimeters to micrometers, and since the phase transformations in the cement paste take place at a broad range of scales, a comprehensive mathematical model for characterizing the degradation of concrete stiffness at elevated temperatures must be a multiscale model which incorporates the chemo-mechanical characteristics of the constituents under high temperatures.

Extensive experimental studies have been performed previously for concrete under high temperatures. Piasta [1] conducted experiments to investigate the thermal deformation of constituents in hardened cement paste and to determine temperatures which initiate the destruction of the microstructure of cement paste in the range of 20–800 °C. Schneider and Herbst [2] and Piasta et al. [3] examined chemical reactions and the behaviors of $Ca(OH)_2$, $CaCO_3$ (calcite), *C-S-H*, non-evaporable water and micropores under various temperatures. In a study conducted by Lin et al. [4] the microstructure of concrete was exposed to elevated temperatures in both actual fire and laboratory conditions and evaluated with the use of Scanning-Electron-Microscopy (SEM) and stereo microscopy. Wang et al. [5] used SEM to examine the cracking of high performance concrete (HPC) exposed to high temperatures and at the same time under axial compressive loading.

Despite the experimental studies, a prediction model has not yet been developed for the degradation of stiffness of concrete in which both temperature dependency and phase transformation of the constituent phases in concrete are taken into account. This study is an innovative attempt to predict the thermal degradation of elastic modulus of concrete considering phase transformations in different temperature ranges. Stoichiometric models are used to characterize the volume changes of the constituents under different temperatures, then composite models are used to obtain effective elastic moduli of the concrete based on the volume changes calculated using the stoichiometric models.

Aggregate plays an important role in the degradation process of concrete under high temperature. Although the study is focused on phase transformations in the cement paste, the effect of different aggregates is included in the model by using appropriate thermal degradation factors.

The internal structure of concrete was divided into the following four scale levels by Constantinides and Ulm [6]:

(a) Level 1 (10^{-8}–10^{-6} m, the *C-S-H* level): A characteristic length scale of 10^{-8}–10^{-6} m is the smallest material length scale. At this scale, *C-S-H* exists in at least two forms with different volume fractions (inner and outer *C-S-H*).

* Corresponding author. Tel.: +1 303 492 8991; fax: +1 303 492 7317.
E-mail address: Yunping.Xi@colorado.edu (Y. Xi).

0008-8846/$ – see front matter © 2009 Elsevier Ltd. All rights reserved.
doi:10.1016/j.cemconres.2009.05.008

(b) Level 2 (10^{-6}–10^{-4} m, the cement paste level): Homogeneous *C-S-H* with large *CH* crystals, aluminates, cement clinker inclusions, and water.
(c) Level 3 (10^{-3}–10^{-2} m, the mortar level): Sand particles embedded in a homogeneous cement paste matrix.
(d) Level 4 (10^{-2}–10^{-1} m, the concrete level): Concrete is a composite material. Coarse aggregates are embedded in a homogeneous mortar matrix.

In this study, the lowest scale is the cement paste level (or Level 2) at the micron scale. The decomposition of *C-S-H* under high temperatures will be included in stoichiometric models.

2. Initial volume fractions of constituents

In order to evaluate the phase transformations in cement paste under high temperatures, we must know the initial volume fractions of the constituents in the cement paste when a high temperature is applied to the concrete. These initial values are related to the degree of hydration of cement particles at the time when the concrete is exposed to the high temperature. Methods to characterize the degree of hydration of cement particles are described in Appendix A. The initial volume fractions of the constituent phases are calculated at two different scale levels: first at the cement paste level by considering only the water-to-cement ratio, and then at the mortar and concrete level by considering the volume fractions of fine and coarse aggregates.

2.1. Initial volume fractions of the constituent phases at the cement paste level

The initial volume fraction of the constituents of cement paste is calculated on the basis of parameters and expressions developed by Bernard et al. [7]. At the cement paste level, the total volume is composed of reactants (remaining water and cement grains) and products of the hydration reactions (such as *C-S-H*, *CH*, products by aluminates, and capillary voids). The total volume is expressed by Eq. (1).

$$V^{\text{total}}_{\text{level\_c.p.}} = V_{\text{w}}(t) + \sum_i V^{\text{ck}}_i(t) + V_{C\text{-}S\text{-}H}(t) + V_{CH}(t) + V_{AL}(t) + V_{\text{capillary voids}}(t) \tag{1}$$

The volume of remaining water in the reactant phases is obtained by subtraction of the water consumed during hydration from the initial water content.

$$V_{\text{w}}(t) = V^{\text{o}}_{\text{w}} - \sum_i V^{i}_{\text{w}} \times \alpha_i(t) \geq 0 \tag{2}$$

V_{w} is the volume of the remaining water, V^{o}_{w} is the initial volume of water in the matrix, and V^{i}_{w} is the volume of the consumed water for complete hydration of clinker *i*. V^{i}_{w} is calculated by Eq. (3).

$$\frac{V^{i}_{\text{w}}}{V^{\text{o}}_{\text{c}}} = N^{i}_{\text{w}} \times \frac{\rho^{*}_i / \mu_i}{\rho_{\text{w}} / \mu_{\text{w}}}\ ;\ \rho^{*}_i = \frac{M_i}{V^{\text{o}}_{\text{c}}} = \rho_{\text{c}} \frac{m_i}{\sum_i m_i} \tag{3}$$

V^{o}_{c} is the initial cement volume, m_i (m_{C_3S}, m_{C_2S}, m_{C_3A}, and m_{C_4AF}) is the mass fraction of clinker phases in the cement, and μ_i is molar mass of phase *i*. Thereby $N^{i}_{\text{w}} = n_{\text{w}}/n_i$ denotes the number, n_{w}, of moles of the consumed water during the hydration of $n_i = 1$ mol of the clinker phase *i* of mass density ρ_i*. For example, the hydration reactions of C_3S and C_2S compound are expressed by Eqs. (4) and (5).

$$2C_3S + 10.6H \rightarrow C_{3.4} - S_2 - H_8 + 2.6CH \tag{4}$$

$$2C_2S + 8.6H \rightarrow C_{3.4} - S_2 - H_8 + 0.6CH \tag{5}$$

In Eq. (4), the ratio of consumed water to the hydration of C_3S is 5.3. Among them, 1.1 mol are chemically bound, 2.9 mol are absorbed in the *C-S-H* pores, and 1.3 mol are consumed to form *CH*. In Eq. (5), the ratio of consumed water to the hydration of C_2S is 4.3. Thus, $N^{C_3S}_{\text{w}}$ and $N^{C_2S}_{\text{w}}$ are 5.3 and 4.3 respectively. Eqs. (4) and (5) also show that the hydration of C_3S and C_2S leads to the formation of 1.3 mol of *CH* and 0.3 mol of *CH* respectively.

Table 1
Parameters for the determination of the volume fractions.

Parameters	Reactants						Products	
	C_3S	C_2S	C_3A	C_4AF	w	c	$C_{3.4}$-S_2-H_8	CH
ρ_i* [g/cm^3]	ρ_{C_3S}*	ρ_{C_2S}*	ρ_{C_3A}*	ρ_{C_4AF}*	1.00	3.15	2.04	2.24
m_i	0.543	0.187	0.076	0.073	–	–	–	–
μ_i [g/mol]	228.32	172.24	270.20	430.12	18	–	227.2	74
$N^{i}_{C\text{-}S\text{-}H}$	1.0	1.0	–	–	–	–	–	–
N^{i}_{CH}	1.3	0.3	–	–	–	–	–	–
N^{i}_{w}	5.3	4.3	10.0	10.75	–	–	–	–

The volume of the hydrated clinker phases in the cement is calculated according to Eq. (6) in which $V^{\text{ck\_o}}_i$ is the initial volume of the clinker phases in the cement.

$$V^{\text{ck}}_i(t) = V^{\text{ck}_{\text{o}}}_i [1 - \alpha_i(t)] \tag{6}$$

C-S-H and *CH* are produced by the hydration of C_3S and C_2S. The volume of *C-S-H* is calculated by Eq. (7).

$$V_{C\text{-}S\text{-}H}(t) = V^{C_3S}_{C\text{-}S\text{-}H} \times \alpha_{C_3S}(t) + V^{C_2S}_{C\text{-}S\text{-}H} \times \alpha_{C_2S}(t) \tag{7}$$

$V^{C_3S}_{C\text{-}S\text{-}H}$ and $V^{C_2S}_{C\text{-}S\text{-}H}$ are asymptotic volumes produced by the hydration of C_3S and C_2S, which are determined by Eqs. (8) and (9) respectively.

$$\frac{V^{C_3S}_{C\text{-}S\text{-}H}}{V^{\text{o}}_{\text{c}}} = N^{C_3S}_{C\text{-}S\text{-}H} \times \frac{\rho^{*}_{C_3S} / \mu_{C_3S}}{\rho_{C\text{-}S\text{-}H} / \mu_{C\text{-}S\text{-}H}};\ \rho^{*}_{C_3S} = \frac{M_{C_3S}}{V^{\text{o}}_{\text{c}}} = \rho_{\text{c}} \frac{m_{C_3S}}{\sum_i m_i} \tag{8}$$

$$\frac{V^{C_2S}_{C\text{-}S\text{-}H}}{V^{\text{o}}_{\text{c}}} = N^{C_2S}_{C\text{-}S\text{-}H} \times \frac{\rho^{*}_{C_2S} / \mu_{C_2S}}{\rho_{C\text{-}S\text{-}H} / \mu_{C\text{-}S\text{-}H}};\ \rho^{*}_{C_2S} = \frac{M_{C_2S}}{V^{\text{o}}_{\text{c}}} = \rho_{\text{c}} \frac{m_{C_2S}}{\sum_i m_i} \tag{9}$$

The volume of *CH* is calculated using Eqs. (10)–(12) in analogy to Eqs. (7)–(9).

$$V_{CH}(t) = V^{C_3S}_{CH} \times \alpha_{C_3S}(t) + V^{C_2S}_{CH} \times \alpha_{C_2S}(t) \tag{10}$$

$$\frac{V^{C_3S}_{CH}}{V^{\text{o}}_{\text{c}}} = N^{C_3S}_{CH} \times \frac{\rho^{*}_{C_3S} / \mu_{C_3S}}{\rho_{CH} / \mu_{CH}} \tag{11}$$

$$\frac{V^{C_2S}_{CH}}{V^{\text{o}}_{\text{c}}} = N^{C_2S}_{CH} \times \frac{\rho^{*}_{C_2S} / \mu_{C_2S}}{\rho_{CH} / \mu_{CH}} \tag{12}$$

The parameters used in these equations are taken from Bernard et al. [7] and are summarized in Table 1. The capillary voids produced by the chemical shrinkage of the hydrates which occur during the hydration can be approximated by Eq. (13) (see, Bentz [8]).

$$V_{\text{capillary voids}} = C_{\text{s}} \cdot \rho_{\text{c}} \cdot V^{\text{o}}_{\text{c}} \cdot \alpha(t) \tag{13}$$

C_{s} is the chemical shrinkage per gram of cement for which the value of 0.07 ml/g is used as suggested by Bentz [8]. All volume fractions are determined with the aid of Eq. (14). $V^{\text{total}}_{\text{level\_c.p.}}$ is the initial volume of the cement and water in the mixture because the value remains constant with time. The fraction of the volume occupied by aluminates is determined using Eqs. (14) and (15).

$$f_i = \frac{V_i}{V^{\text{total}}_{\text{level\_c.p.}}} = \frac{V_i}{V^{\text{o}}_{\text{c}} + V^{\text{o}}_{\text{w}}} = V_i / V^{\text{o}}_{\text{c}} \cdot \left(1 + \frac{\rho_{\text{c}}}{\rho_{\text{w}}} \cdot \frac{w}{c}\right) \tag{14}$$

$$f_{AL} = 1 - \left(f_{C\text{-}S\text{-}H} + \sum_i f_i^{ck} + f_{CH} + f_w + f_{\text{capillary voids}} \right) \quad (15)$$

Under the condition of complete hydration ($\alpha = 1$), the volume fractions of the cement paste, with w/c ratios of 0.5 and 0.67, are summarized in Table 2. In the cement paste with w/c ratio of 0.5, the remaining water and capillary void form a macroporosity of 14.84% ($f_{\text{capillary void}} + f_w = 14.84\%$). These values agree with the results from Taylor [9] and Hansen [10] quite well. Note the w/c ratio of 0.67 is being used for residual compression tests which were performed in-house in the present study.

2.2. Initial volume fractions of the constituent phases at the mortar and concrete levels

The volume fractions of the constituent phases at the mortar and concrete levels are related to the mass proportions of the concrete mix design. At the mortar level, the volume fractions of the cement paste and sand can be calculated from Eq. (16).

$$f_s = \frac{f_s^o}{f_c^o + f_w^o + f_s^o} = \frac{u_s/\rho_s}{u_c/\rho_c + u_w/\rho_w + u_s/\rho_s};\ f_{cp} = 1 - f_s \quad (16)$$

u_c, u_w, and u_s are the different masses per unit volume of cement, water, and sand respectively. ρ_c, ρ_w, and ρ_s are the mass densities of cement, water, and sand respectively. f_{cp} and f_s are the volume fractions of cement paste and sand in mortar respectively. The volume fractions at the concrete level are obtained by considering the coarse aggregate (gravel) in Eq. (17).

$$f_g = \frac{f_g^o}{f_c^o + f_w^o + f_s^o + f_a^o} = \frac{u_g/\rho_g}{u_c/\rho_c + u_w/\rho_w + u_s/\rho_s + u_g/\rho_g};\ f_m = 1 - f_g \quad (17)$$

where u_g is the mass of coarse aggregate per unit volume and ρ_g is the mass density of coarse aggregate. f_m and f_g are the volume fractions of mortar and coarse aggregate in concrete respectively.

3. A multiscale stoichiometric model for phase transformations in concrete exposed to high temperatures

3.1. Phase transformations at the cement paste level

The initial volume fractions of constituents in concrete will change when the concrete is exposed to high temperature. The changes of the volume fractions can be characterized by considering the phase transformation in the concrete under different ranges of high temperature. However, it is difficult to calculate each phase transformation exactly with temperature increase because, with respect to temperature increase, some of the stoichiometric reactions have not yet been completely established based on experimental data. Therefore, some hypotheses need to be made to predict the phase transformations involved in concrete under high temperature. In the present model, the following assumptions are used.

The first assumption is that the total volume of hardened cement paste is considered as a constant, that is, the total volume of the components before phase transformations take place is the same as the total volume of the components after the phase transformation. In fact, the total volume varies under different temperatures (Bazant and Kaplan [11]), which will be discussed in detail later.

Table 2
Volume fractions of constituents at cement paste level ($w/c = 0.5$ and 0.67).

Volume fractions	% ($w/c = 0.5$)	% ($w/c = 0.67$)
$f_{C\text{-}S\text{-}H}$	53.69	44.45
f_{CH}	15.71	13.01
f_{AL}	15.76	13.04
$f_{\text{capillary void}}$	8.56	7.09
f_w	6.28	22.41

Table 3
Processes of decomposition depending on the temperature regime.

Temperature	Decomposition
20–120 °C	Evaporation of free water, dehydration of *C-S-H* and ettringite
120–400 °C	Dehydration of *C-S-H*
400–530 °C	Dehydration of *C-S-H*, dehydration of *CH*
530–640 °C	Dehydration of *C-S-H*, decomposition of poorly crystallized $CaCO_3$
640–800 °C	Dehydration of *C-S-H*, decomposition of $CaCO_3$

The second assumption is that volume fractions of the constituents in cement paste are assumed as linear functions of temperature during the phase transformations, and they vary linearly between the beginning and ending temperature. For instance, *C-S-H* is decomposed continuously and proportionally from room temperature up to 800 °C. The free water is evaporated at about 100–120 °C and bound water is gradually released up to 800 °C. The loss of the bound water is assumed to be a linear function between 100 °C and 800 °C.

The third assumption is that the loss of carbonation between 600 °C and 900 °C and the decrease of calcite ($CaCO_3$) between 600 °C and 800 °C are neglected in the present model because their effects on concrete stiffness are relatively small.

The last assumption is that the aluminum hydrates are regarded as non-reactive substances regardless of temperature increase.

The capillary void, the remaining water, and the water in gel pores are regarded as the initial total void at the cement paste level.

$$f_{\text{void\_cement}} = f_w + f_{\text{capillary void}} + f_{\text{water in gel pores}} \quad (18)$$

According to Copeland and Bragg [12], the volume of water in gel pores is about 28% of the total volume of the gel. Therefore, the volume of the water in gel pores is considered as 28% of *C-S-H* volume.

Since the water in the gel pores is assumed as the initial void, it should be noted that Eqs. (4) and (5) are balanced assuming all of the hydration products are saturated. After evaporation of free water in gel pores, the chemical formula of *C-S-H* is regarded as $C_{3.4}$-S_2-H_3 (Tennis and Jennings [13]). This means that 5 mol of H_2O (free water in gel pores) per 1 mol of *C-S-H* is evaporated between 100 and 120 °C. Thus, after evaporation of free water in gel pores, the decomposition of *C-S-H* is described by Eq. (19). Between 400 °C and 530 °C, the decomposition of calcium hydroxide (*CH*) is expressed using Eq. (20).

$$3.4CaO \cdot 2SiO_2 \cdot 3H_2O \rightarrow 3.4CaO \cdot 2SiO_2 + 3H_2O\uparrow \quad (19)$$

$$Ca(OH)_2 \rightarrow CaO + H_2O \quad (20)$$

The volume of water decomposed from *C-S-H* and *CH* is regarded as additional void. It is assumed that *CH* and *C-S-H* are completely decomposed at 530 °C and 800 °C, respectively. Under this assumption the volume fraction of the decomposed total water from *C-S-H* (between 120 and 800 °C) and *CH* (between 400 and 530 °C) is calculated using Eq. (21).

$$f_i^w = f_i \times N_w^i \times \frac{\rho_i/\mu_i}{\rho_w/\mu_w} \quad (21)$$

f_i^w is the volume fraction of water decomposed from phase i [$i = C_{3.4}S_2H_3$ and *CH*] in the cement paste. f_i is the initial volume fraction of phase i. Particularly, it should be noted that $f_{C\text{-}S\text{-}H}$ is the volume fraction after evaporation of the free water in *C-S-H* gel pores. $N_w^i = n_w/n_i$ denotes the value n_w as a number of moles of water decomposed from $N_i = 1$ mol of phase i ($N_w^{C\text{-}S\text{-}H} = 3.0$ and $N_w^{CH} = 1.0$). The density and molar mass of

Table 4
Theoretical formulas for volume fraction change of each phase ($w/c = 0.67$).

Temperature	Formulas (%)
120 °C ≤ T ≤ 800 °C	$f_{C_{3.4}S_2H_3} = -4.70612010\ 10^{-2}T + 37.648961$
	$f_{C_{3.4}S_2} = 3.4876827\ 10^{-2}T - 4.185224$
	$f^{w}_{C_{3.4}S_2H_3} = 1.21843383^{-2}T - 1.462121$
400 °C ≤ T ≤ 530 °C	$f_{CH} = -1.00053064\ 10^{-1}T + 53.028124$
	$f_{CaO} = 4.55376650\ 10^{-2}T - 18.215066$
	$f^{w}_{CH} = 5.45153994\ 10^{-2}T - 21.806160$

$C_{3.4}S_2H_3$ are 1.75 g/cm^3 and 365 g/mol respectively (Tennis and Jennings [13]). The parameters for *CH* and water are listed in Table 1.

Finally, the volume of calcium oxide (*CaO*) produced from the decomposition of *CH* is obtained by deducting the decomposed water volume from initial volume of *CH*. From the same methodology, the volume of $C_{3.4}S_2$ produced from the decomposition of $C_{3.4}S_2H_3$ is obtained by deducting the decomposed water volume from the initial volume of $C_{3.4}S_2H_3$.

Different processes of decomposition obtained from literature are summarized in Table 3 with respect to different temperature ranges (from 20 °C to 800 °C). The theoretical formulas for the change of volume fraction of each phase considering temperature ranges and w/c ratio are obtained from schemes described above. Table 4 shows the theoretical formulas of each phase in cement paste with a w/c ratio of 0.67 for the given temperature ranges. Fig. 1 shows the result for the change of volume fraction with the transformations of each phase up to 800 °C using the formulas presented in Table 4.

3.2. Validation of the present model at cement paste level

There has been no systematic quantitative measurements considering changes of all the phases (*C-S-H*, *CH*, *CaO*, solid grains, and so on) in cement paste with respect to temperature increase. Thus, the validation of the present model is done by (i) using the variation of pore volume under elevated temperatures measured experimentally by Piasta et al. [3], and (ii) comparing the theoretical calculation for the porosity change by Harmathy [14].

Piasta et al. [3] performed various experimental studies related to the thermal properties of concrete with w/c of 0.4 at elevated temperatures. Harmathy [14] calculated the porosity, the true density, and the bulk density of an idealized cement paste with w/c of 0.5 at elevated temperature using formulas based on the work of Powers [15]. Table 5 shows the mass fractions of clinker phases for the cements used in the experiments of Piasta et al. [3] and the theoretical calculation of Harmathy [14]. Table 6 shows the result of porosity tests between 20 °C and 800 °C by Piasta et al. [3].

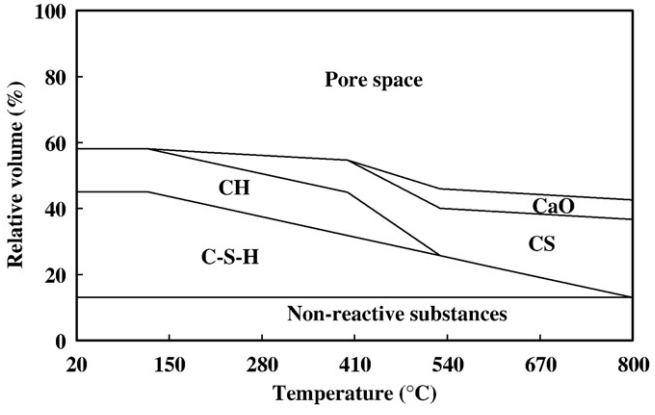

Fig. 1. Change of phase composition with increasing temperature ($w/c = 0.67$).

Table 5
Mass fractions of clinker phases in the cement.

Clinker phases	m_{C_3S}	m_{C_2S}	m_{C_3A}	m_{C_4AF}	Others
Piasta et al. [1]	0.632	0.154	0.099	0.080	0.035
Harmathy [14]	0.470	0.270	0.116	0.090	0.054

To compute the volume fraction of the voids in cement paste from the test data of Piasta et al. [3], the density of cement paste is approximated using Eq. (22).

$$\rho_{cp} = \frac{m_{cp}}{V_{cp}} = \frac{m_w + m_c}{V_w + V_c} = \frac{\rho_c \cdot (1 + w/c)}{1 + (\rho_c/\rho_w) \cdot (w/c)} \tag{22}$$

The volume fraction of the voids from the test data is calculated as the product of the density of cement paste using Eq. (22) and the value of total porosity. In Eq. (2), $V_w(t)$ has a positive value beyond the w/c ratio of 0.45 for the cement used in their test. For w/c ratio of 0.4, the volume fraction of completely hydrated cement compounds is 0.89. The remaining 11% of cement compounds exists as solid grains (non-reactive substances) in the cement paste. To reflect this volume fraction of completely hydrated grains in Eqs. (2), (7), (10), and (13), $\alpha_i(t)$, the degree of hydration, is multiplied by the factor of 0.89 for these equations. The remaining procedures are the same as discussed above.

The comparison for pore volume fractions between the present model and the test data by Piasta et al. [3] is shown in Fig. 2. It can be seen clearly that the present model predicts the test results by Piasta et al. [3] very well. The comparison between the present model and the theoretical calculation by Harmathy [14] is shown in Fig. 3. It is evidenced that the difference between the present model and the model by Harmathy [14] is quite large. This is because the model of Harmathy [14] assumed that cement was only composed of C_3S (0.653 as the weight fraction) and C_2S (0.365 as the weight fraction). In other words, for the prediction of voids in a cement paste, Harmathy's model only considered two phases (*C-S-H* and *CH*), which are formed from the C_3S and C_2S components, as the total volume of cement paste. This assumption might cause a larger error than the present model because the model overestimates the volume of voids with respect to temperature increase.

3.3. The volume fractions of the phases at the mortar and concrete levels

At an elevated temperature, aggregates expand. However, the expansion is small compared to the initial volume. Therefore, the total

Table 6
Porosity and pore size distribution ($w/c = 0.4$, Piasta et al. [3]).

Property	Temperature (°C)								
	20	100	20	300	400	500	600	700	800
Total porosity (cm^3/g)	0.101	0.116	0.115	0.122	0.135	0.147	0.211	0.245	0.223
Mercury porosity (cm^3/g)	0.083	0.098	0.089	0.105	0.109	0.107	0.153	0.189	0.159
Percentage of pores in radius intervals									
5–10 (nm)	10	6.7	4	5.1	4.6	3.6	2.4	4.1	1.6
10–15	6.4	6.7	5.4	6.5	5.4	3.8	3.7	3.7	3.3
15–25	10.4	11.3	11.7	9.9	13.4	10.3	10.6	7.8	7
25–50	17.7	25.1	242	16	21.3	20.4	20.4	17.6	16.1
50–75	10.2	19.5	20.2	12.5	14.1	17.5	15.4	12.7	12.9
75–100	5	6.6	7.7	5.3	5.8	7.4	6.4	5.9	7
100–150	7.2	6.6	7.9	6.3	7.5	8.2	8	6.5	7.7
150–250	18.9	12.9	12.5	14.4	15.3	14.4	12.5	10.4	11.7
250–500	11.2	3.8	5.8	20.1	10.3	11	16.7	26.1	21.3
500–1000	2	0.2	1.8	2.3	1.6	2.2	2.9	4.3	10.5
1000–7500	0.8	0.1	0.9	1.1	0.7	1.2	1.1	1	0.9

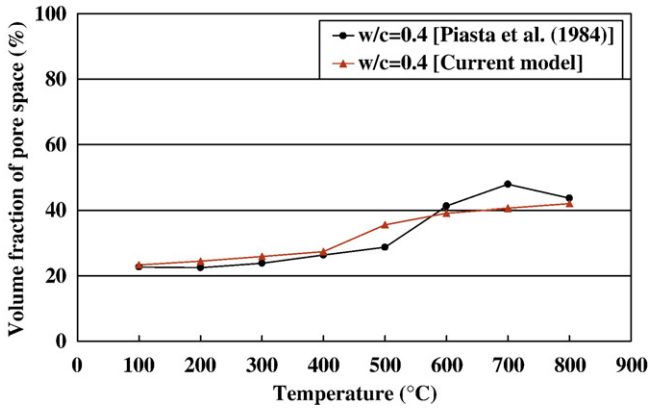

Fig. 2. Comparison between the current model and test data by Piasta et al. [3].

volume of aggregates is assumed to be constant in the calculation for the volume fractions of sand and gravels.

The volume fractions of each phase with respect to temperature increase at the mortar and concrete levels are calculated with Eqs. (23) and (24).

$$f_{i'\_\text{mortar}} = f_i \cdot f_{\text{cp}\_\text{mortar}};\ f_{\text{s}\_\text{mortar}} = f_{\text{s}},\ \text{at mortar level} \tag{23}$$

$$f_{i'\_\text{con}} = f_i \cdot f_{\text{cp}} \cdot f_{\text{m}};\ f_{\text{s}\_\text{con}} = f_{\text{s}} \cdot f_{\text{m}};\ f_{\text{g}\_\text{con}} = f_{\text{g}},\ \text{at concrete level} \tag{24}$$

In which, f_i is the volume fraction for $C_{3.4}S_2H_3$, *CH*, *AL*, $C_{3.4}S_2$, *CaO*, and void_cement which changed with temperature increase at the cement paste level. Tables 7 and 8 show volume fractions of each phase at the mortar level and concrete levels respectively (for $w/c = 0.67$).

4. Thermal degradation of the modulus of elasticity of concrete

A recently developed theory of composite damage mechanics (Xi [16]; Xi and Nakhi [17]; Xi et al. [18]) is used in this study for handling the effect of phase transformations on stiffness of concrete. The changes in volume fractions of the constituents in concrete result in variation of stiffness of the concrete, which can be modeled by the following equation as an effective modulus, E_{eff}, of a two-phase composite

$$E_{\text{eff}} = f_j(c_2)E_1 \tag{25}$$

in which E_1 is the modulus of phase 1 (may be considered as the matrix) and c_2 is the volume fraction of phase 2 (may be considered as the inclusion). The total volume, V, contains volume V_1 for phase 1 and volume V_2 for phase 2, in such a manner that $V_1 + V_2 = V$.

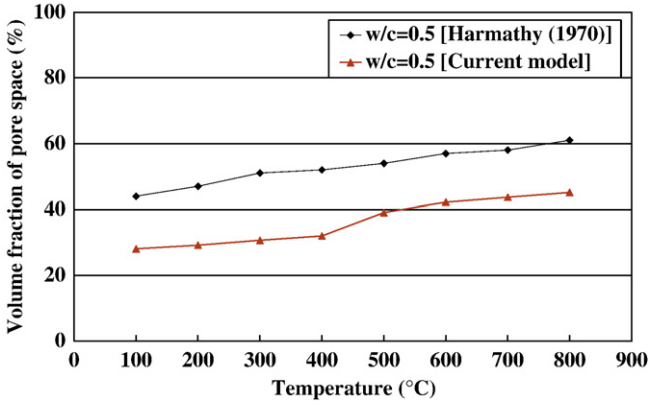

Fig. 3. Comparison between the current model and model of Harmathy [14].

Table 7
Volume fraction of phases at mortar level ($w/c = 0.67$).

Volume (%)	Temperature (°C)				
	20 °C≤T≤120 °C	200 °C	400 °C	600 °C	800 °C
$C_{3.4}S_2H_3$	16.87	14.88	9.92	4.96	0.00
$C_{3.4}S_2$	0.00	1.47	5.15	8.82	12.50
CH	6.86	6.86	6.86	0.00	0.00
CaO	0.00	0.00	0.00	3.12	3.12
AL	6.88	6.88	6.88	6.88	6.88
void_cement	22.11	22.62	23.91	28.93	30.21
Sand	47.29				

Depending on the volume fraction and distribution of phase 2 in phase 1, $f_j(c_2)$ represents the variation of the effective modulus due to the appearance of phase 2. Subscript j represents different distributions of phase 2 in the two-phase composite. If phase 2 is distributed in the form of spherical shapes of different sizes and distributed randomly within phase 1, $f_j(c_2)$ can be expressed by Eq. (26).

$$f_{\text{spherical}}(c_2) = 1 + \frac{c_2}{(1-c_2)/3 + 1/[(E_2/E_1) - 1]} \tag{26}$$

Eq. (26) is called the spherical composite model or the generalized self-consistent model for the effective modulus of a two-phase composite.

When phase transformations take place in concrete under high temperatures some phases with high moduli convert to other phases with lower moduli or with zero moduli (such as voids). Nucleation of voids in this case, is due to evaporation of water at high temperature. Water includes the initially remaining water in the concrete as well as the water generated by phase transformations. To describe the effect of phase transformations taken place under high temperatures, we assume that the transformed phases in the concrete are generated randomly in spherical shapes of different sizes within the original phases. So, Eqs. (25) and (26) can be used to calculate the effective modulus of concrete under various temperatures.

4.1. Thermal degradation at the cement paste level

Considering the phase transformations as independent processes (they may take place simultaneously but without coupling), the expression for the effective modulus in Eq. (27) can be developed based on the composite damage mechanics (Xi and Nakhi [17]; Xi et al. [18]) Eq. (25).

$$\begin{aligned} E_{\text{eff}}^{T} &= f_{\text{spherical}}^{T,i} E_{\text{con\_ref}} = \left(f_{\text{spherical}}^{T,C_{3.4}S_2H_3} \cdot f_{\text{spherical}}^{T,CH} \cdots\right) \cdot E_{\text{con\_ref}} \\ &= \left(\prod_{i=C_{3.4}S_2H_3}^{N} f_{\text{spherical}}^{T,i}\right) \cdot E_{\text{con\_ref}} \end{aligned} \tag{27}$$

in which the function $f_{\text{spherical}}^{T,i}$ denotes the thermal degradation factor of the elastic modulus from each original phase to their respective decomposed state. Eq. (27) is a result of recursive applications

Table 8
Volume fraction of phases at concrete level ($w/c = 0.67$).

Volume (%)	Temperature (°C)				
	20 °C≤T≤120 °C	200 °C	400 °C	600 °C	800 °C
$C_{3.4}S_2H_3$	10.71	9.45	6.30	3.15	0.00
$C_{3.4}S_2$	0.00	0.93	3.27	5.60	7.93
CH	4.35	4.35	4.35	0.00	0.00
CaO	0.00	0.00	0.00	1.98	1.98
AL	4.36	4.36	4.36	4.36	4.36
void_cement	14.03	14.36	15.17	18.36	19.18
Sand	30.02				
Gravel	36.53				

of Eq. (25), with each transformation described by its own function $f^{T,i}_{\text{spherical}}$ For example, $C_{3.4}S_2H_3$ decomposes into $C_{3.4}S_2$ and H_2O (considered as new void) with increasing temperature as shown in Eq. (19); c_2 is the volume fraction of the decomposed phase $C_{3.4}S_2$ with respect to the original phase $C_{3.4}S_2H_3$, and E_2/E_1 is the ratio for the elastic modulus of the decomposed phase $C_{3.4}S_2$ (E_2) to the original phase $C_{3.4}S_2H_3$ (E_1). The effective stiffness is obtained by inserting Eq. (26) into Eq. (25) considering the original phase $C_{3.4}$-S_2H_3 and the decomposed phase $C_{3.4}S_2$.

To obtain the finalized thermal degradation factor for the original phase $C_{3.4}S_2H_3$, Eq. (26) is applied again for the second decomposed phase H_2O. In Eq. (26), the stiffness of the original phase, E_1, is the effective stiffness $E^{C_{3.4}S_2\_C_{3.4}S_2H_3}_{\text{eff}}$, which is obtained from $C_{3.4}S_2H_3$ and the previous transformation $C_{3.4}S_2$. The volume fraction and stiffness of H_2O (new void) phase are c_2 and E_2 (where the new phase is a void with $E_2=0$). Eq. (28) is the function for the thermal degradation factor of the elastic modulus transformed from $C_{3.4}S_2H_3$ (the original phase) to $C_{3.4}S_2$ and H_2O (the respective decomposed phases).

$$f^{T,C_{3.4}S_2H_3}_{\text{spherical}} = 1 + \frac{c_{H_2O}}{\left(1-c_{H_2O}\right)/3 + 1/\left[\left(E_{H_2O}/E^{C_{3.4}S_2C_{3.4}S_2H_3}_{\text{eff}}\right)-1\right]} \quad (28)$$

In the application of the composite damage mechanics, it is noticed that E_{eff} obtained from the first decomposed phase should be higher than the elastic modulus of the second decomposed phase because the thermal degradation factor should always be less than or at most equal to 1. In summary, the modulus ratios in $f^{T,i}_{\text{spherical}}$ are not simply the stiffness ratios of the product and the reactant, but the stiffness ratios of the product and the effective media.

4.2. Thermal degradation at the mortar and concrete levels

It is important to point out that Eq. (27) does not include the effects of aggregates on stiffness of concrete, such as thermal degradation of aggregate and debonding between aggregate and cement paste. The aggregates themselves may experience various phase changes during different heating and cooling rates. Moreover, concrete expands during heating up to about 150 °C; the maximum expansion is 0.2%. No further expansion occurs between 150 and 300 °C. Between 300 °C and 800 °C the hardened cement paste shrinks, and the shrinkage is between 1.6 and 2.2% at 800 °C. The expansion and shrinkage of cement paste have three different impacts on properties of concrete. First, they do not match with the expansion of aggregate in concrete under elevated temperature, and thus generate cracks and debonding in concrete, which lower the stiffness of concrete. This type of impact will be considered in this section. Second, the expansion and shrinkage of cement paste affect the coefficient of thermal expansion of the concrete, which will be addressed by another paper by the authors. The third impact is that.

Table 9
Elastic properties of constituent phases.

Phases	E (Gpa)	ν (–)	References
CSH	31 ± 4	–	Acker [19]
	29.4 ± 2.4	0.24	Constantinides and Ulm [6]
C_3S	135 ± 7	0.3	Acker [19]
	147 ± 5	0.3	Velez et al. [20]
C_2S	140 ± 10	0.3	Acker [19]
	130 ± 20	0.3	Velez et al. [20]
CH	35.24	–	Beaudoin [21]
	48	–	Wittmann [22]
	39.77–44.22	0.305–0.3	Monteiro and Chang [23]
	36 ± 3		Acker [19]
	38 ± 5	–	Constantinides and Ulm [6]
CaO	194.54 ± 0.5	0.207	Oda et al. [24]
C_3A	160 ± 10	–	Acker [19]
	145 ± 10	–	Velez et al. [20]
C_3AF	125 ± 25	–	Velez et al. [20]

they change the volume of the concrete to a certain extent, but the variation is quite small compared with the total volume. Therefore, the total volume of the cement paste can be assumed as a constant in Section 3.1.

To take into account the effects of the mismatch between the deformations of cement paste and aggregate, another function, $f_{\text{agg\_deg}}$ is introduced in the model. Eqs. (29) and (30) define the final thermal degradation function for the elastic modulus of concrete. Eq. (30) represents the total thermal degradation factor of concrete.

$$E^T_{\text{eff}} = \left(\prod_{i=C_{3.4}S_2H_3}^{N} f^{T,i}_{\text{spherical}}\right)\cdot f_{\text{agg\_deg}}\cdot E_{\text{con\_ref}} = F(T)E_{\text{con\_ref}} \quad (29)$$

$$F(T) = \left(\prod_{i=C_{3.4}S_2H_3}^{N} f^{T,i}_{\text{spherical}}\right)\cdot f_{\text{agg\_deg}} \quad (30)$$

$f_{\text{agg\_deg}}$ includes the combined effect of aggregate on stiffness of concrete. Because of the lack of detailed experimental data, $f_{\text{agg\_deg}}$ is obtained from a regression curve from test data shown in Bazant and Kaplan [11]. As the first approximation, the $f_{\text{agg\_deg}}$ as shown Eq. (31) incorporates the effects of interface cracks and debonding between aggregates and hardened cement paste and the thermal degradation of aggregates themselves.

$$f_{\text{agg\_deg}} = 0.03921 + e^{-0.002T} \quad (31)$$

The effect of Eq. (31) on the prediction model will be shown in the next section together with the comparisons for experimental results.

5. Comparison between the present model and experimental results

To calculate the thermal degradation of elastic modulus of concrete using the present model, the stiffness of each phase must be evaluated. Table 9 summarizes the elastic properties of the constituent phases obtained from literature.

It is noticed that the elastic moduli of *CS* decomposed from *C-S-H* and *CaO* decomposed from *CH* vary depending on the porosity of the phases. The porosities of *CaO* and $C_{3.4}S_2$ are therefore calculated using the volume fractions of the phases decomposed from *CH* and $C_{3.4}S_2H_3$. The functions are shown in Eq. (32).

$$p_{CaO} = \frac{f_{H_2O\_CH}}{f_{CaO\_CH}+f_{H_2O\_CH}};\ p_{C_{3.4}S_2} = \frac{f_{H_2O\_C_{3.4}S_2H_3}}{f_{C_{3.4}S_2\_C_{3.4}S_2H_3}+f_{H_2O\_C_{3.4}S_2H_3}} \quad (32)$$

Table 10 is a summary for the elastic modulus of each phase used in the present model. The functions for the elastic moduli of *CaO* and $C_{3.4}S_2$ with respect to porosity are based on empirical expressions by Velez et al. [20]. The fixed variable (n) in the function, see Table 10, for the elastic modulus of *CaO* is assumed as 4, which is an average value for variables used in the functions for C_2S and C_2A by Velez et al. [20]. $f^{T,AL}_{\text{spherical}}$ for

Table 10
Elastic moduli of each phase used in the present model.

Phases	p_i (porosity)	E (Gpa)
$C_{3.4}S_2H_3$	–	32.0
$C_{3.4}S_2$	0.26	29.79 [from $E=120\,(1-p_{C_{3.4}S_2})^n$, $n=4.65$]
CH	–	40.2
CaO	0.54	8.35 [from $E=194.54\,(1-p_{CaO})^n$, $n=4$]
Void	–	0

aluminum hydrates is 1 because they were assumed to be a non-reactive substance. Thus, the elastic moduli of aluminum hydrates are not used in the calculation of the thermal degradation.

Finally, the prediction model for the thermal degradation of elastic modulus of concrete can be expressed in terms of temperature, combining the relevant equations in previous sections. The thermal degradation factor of concrete for 20–120 °C is the same as the thermal degradation (f_{agg_deg}) for the elastic modulus of the aggregates because the capillary void, remaining water, and water in gel pores of *C-S-H* are assumed as the initial total void from 20 °C to 120 °C in the model, which means no phase transformation (no damage) up to 120 °C (see Fig. 1). Eqs. (33)–(35) are the thermal degradation factors of concrete for three temperature ranges.

For 120–400 °C,

$$F(T)=\frac{\left(39.21\cdot 10^{-3}+e^{-0.002T}\right)\cdot\left(697.126\cdot 10^{-3}-253.828\cdot 10^{-6}T\right)}{\left(651.437\cdot 10^{-3}+126.914\cdot 10^{-6}T\right)}. \tag{33}$$

For 400–530 °C,

$$F(T)=\frac{\left[563.948\cdot 10^{4}\cdot\left(3.921\cdot 10^{-2}+e^{-0.002T}\right)\cdot\left(178.434\cdot 10^{-2}-279.418\cdot 10^{-5}T\right)\cdot\left(697.126\cdot 10^{-3}-253.828\cdot 10^{-6}T\right)\right]}{(77.1825+T)\cdot(5132.91+T)}. \tag{34}$$

For 530–800 °C,

$$F(T)=\frac{357.689\cdot 10^{-3}\cdot\left(3.921\cdot 10^{-2}+e^{-0.002T}\right)\cdot\left(697.126\cdot 10^{-3}-253.828\cdot 10^{-6}T\right)}{\left(651.437\cdot 10^{-3}+126.914\cdot 10^{-6}T\right)}. \tag{35}$$

The above three equations are functions of temperature only, but they are developed taking into account phase transformations and stiffness degradations in concrete. They represent normalized ratios of the moduli of distressed concrete to the moduli of original concrete in different temperature ranges. The concrete mix design parameters, such as w/c, are included in the parameter E_{con_ref} in Eq. (29).

The prediction model is compared with test data from previous researches including our own study (Lee et al. [25]). Fig. 4 shows the comparison between the present model and the test data. In Fig. 4, the vertical axis is for the relative elastic modulus, which is the ratio, E^T_{eff}/E_{con_ref}. The ratio is used to normalize the test data of different concrete mix design parameters. As one can see from Fig. 4 that the present model satisfactorily predicts the trend of the test results in spite of the fact that the experimental conditions used in previous researches differ from each other, such as w/c ratios, curing ages, heating rates, holding times at each target temperature, and loading time (unstressed test and residual test). In short the model reproduces test results with relatively good accuracy.

As a comparison, Fig. 5 shows the effect of aggregate, which is the curve for Eq. (31); and the effects of phase transformations in cement paste without the effect of aggregate, which are the curves for Eqs. (33)–(35) without combining with Eq. (31).

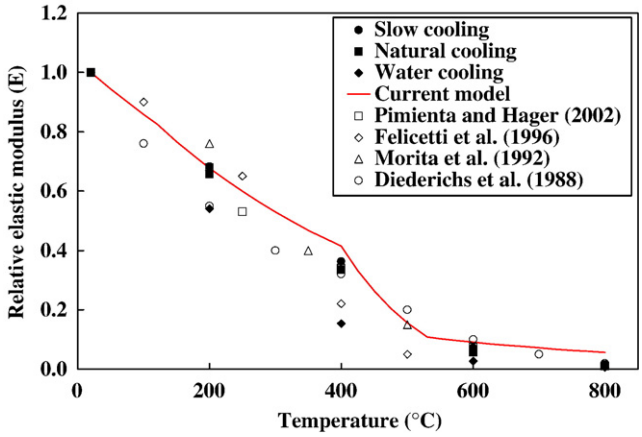

Fig. 4. Comparison between the current model and test data.

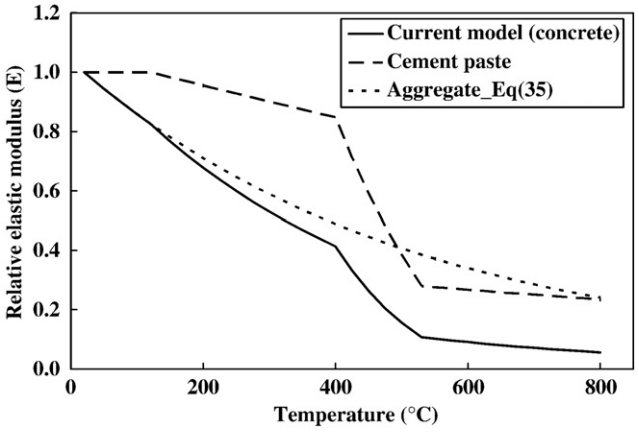

Fig. 5. Comparison of cement, aggregate, and concrete.

6. Conclusions

A multiscale model was established to predict the thermal degradation of the modulus of elasticity of concrete at elevated temperature ranges. The internal structure of concrete was considered at three scale levels: cement paste, mortar, and concrete. Thereby the cement paste is a multi-phase composite with cement particles and the principal hydration products; mortar is a mixture of cement paste and sand; and concrete is a mixture of mortar and gravel.

At the cement paste level, the phase transformations under high temperature were modeled by stoichiometric relations, which furnish the volume fractions of the products of the phase changes. The effective elastic modulus of cement paste under a certain temperature was determined based on composite mechanics models and using the volume fractions of the constituents at the given temperature. The water released during the heating process is considered as part of the pore distribution with zero modulus of elasticity.

The variation of pore volume with increasing temperature was predicted by the present model, and compared with the test data by Piasta et al. [3]. The present model predicted the test results very well.

At the mortar and concrete levels, the effective elastic moduli of mortar and concrete for a given temperature was determined based on composite models using the volume fractions and moduli of cement paste, sand, and gravel. The elastic modulus of cement paste came from the effective modulus obtained from the lower level model, and the variations of elastic moduli of various sand and gravels were established based on available test data in the literature.

The present model for the thermal degradation of elastic modulus of concrete closely reproduced the basic trend of available test results which included various concrete mix design parameters as well as heating and cooling conditions.

The multiscale chemo-mechanical model provided a general framework that can be used to predict for thermal degradations of the elastic modulus as well as other properties of concrete, such as thermal expansion and diffusivity of concrete under high temperatures.

Acknowledgements

The authors wish to acknowledge partial support by the US National Science Foundation under grant CMS-0409747 to the University of Colorado at Boulder. Opinions expressed in this paper are those of the authors and do not necessarily reflect those of the sponsor. The authors also thank Evan Sheesley for his work in editing this paper.

Appendix A. Hydration kinetics model

Typically in Portland cement four clinkers (C_3S, C_2S, C_3A, and C_3AF) participate in the hydration reaction of cement. The hydration process takes place in five periods, namely the initial reaction period (Period 1), the induction period (Period 2), the acceleration period (Period 3), the deceleration period (Period 4), and the slow period (Period 5). Periods 1 and 2 correspond to the early stage of hydration reaction, Periods 3 and 4 to the middle stage, and Period 5 to the late stage (Taylor [9]). The hydration reactions of cement are classified as two processes: The first one is the reaction process of nucleation and growth of the clinker phases, which takes place over 0–20 h. The second is a diffusion controlled process where the kinetics of the hydration reaction is controlled by the rate of diffusion of dissolved ions through the layers of hydrates, which are formed around the clinker. This process develops at ages of 1 day and beyond. The rate of hydration of the second process depends strongly on the water-to-cement (w/c) ratio (Berliner et al. [26]). Fig. A1 is a schematic for the hydration process of cement paste. Eq. (A1) is commonly employed to model the nucleation and growth reaction kinetics in cement chemistry which amounts to the first 20–30% of the reaction:

$$-\ln\left[1-(\alpha_i-\alpha_{oi})\right]=\left[k(t-t_o)^m\right] \tag{A1}$$

α_i is the hydration degree of reaction of clinker i at the time t. α_{oi} is the hydration degree of reaction of clinker i at the time t_o, when the nucleation and growth process dominate the hydration. k is a rate constant that considers the effects of nucleation, multi-dimensional growth, geometric shape factors, and the diffusion process. m is the exponent defining the reaction order. Taylor [27] proposed Eq. (A2), which is a simplification of Eq. (A1)

$$\alpha_i=1-\exp\left[-a_i(t-b_i)^{c_i}\right] \tag{A2}$$

a_i, b_i, and c_i are coefficients, which were determined empirically for the specific Portland cement. The coefficients are shown in Table A1. Also, Eq. (A2) is used as an approximation for long-term hydration reactions of cement paste.

For $t>1$ day, the hydration reactions are controlled by the rate of diffusion, which has been addressed by Berliner et al. [26], and Fuji and Kondo [28]. According to Fuji and Kondo [28], the rate of hydration reaction is

$$(1-\alpha_i)^{1/3}=-(2D_i)^{1/2}(t-t^*)^{1/2}/R+(1-\alpha_i^*)^{1/3} \tag{A3}$$

where α_i^* is the degree of reaction of clinker i at the time t^*. The hydration reactions of the cement particles are governed by the rate of diffusion of dissolved ions. D_i is the diffusion constant (cm^2/h) of clinker i, and R is the initial radius of the clinker grains. An average particle size 2×10^{-6} in. (5×10^{-4} cm) can be used as the initial radius of the clinker grains (R).

The parameter D_i and coefficients taken from Berliner et al. [26] and Bernard [7] are summarized in Table A2. The hydration reaction of the cement paste based on the diffusion theory is very fast as compared with that from the empirical equation, Eq. (A2). The overall degree of hydration, α, of the cement-based material systems is

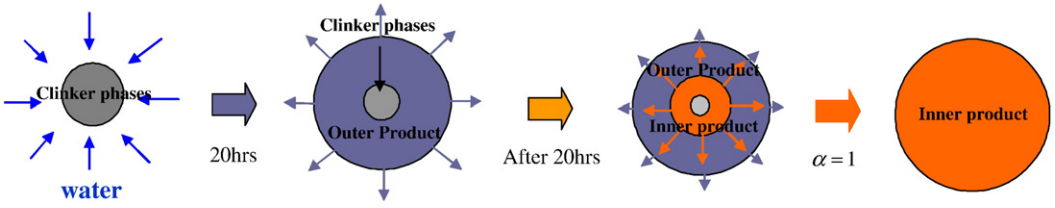

Fig. A1. Hydration process of cement paste.

related to the individual degree of hydration of clinkers. The overall degree of hydration may be expressed by Eq. (A4).

$$\alpha(t) = \frac{\sum_i m_i \alpha_i(t)}{\sum_i m_i} \quad \text{(A4)}$$

$m_i = m_{C_3S}$, m_{C_2S}, m_{C_2A} and m_{C_4AF} are the mass fractions of the clinker phases in the cement.

Table A1
Coefficients of α_i, b_i, and c_i.

Compound	α_i	b_i	c_i
C_3S	0.25	0.9	0.7
C_2S	0.46	0.0	0.12
C_3A	0.28	0.9	0.77
C_3AF	0.26	0.9	0.55

Table A2
Diffusion constant and coefficients in the diffusion model.

Clinkers	w/c	Diffusion model		
		D_i (cm^2/h)	t^* (h)	α_i^*
C_3S	0.3	0.42×10^{-10}	20 or 30	0.60
	0.5	2.64×10^{-10}		
	0.7	15.6×10^{-10}		
C_2S	0.3	6.64×10^{-10}		
	0.5			
	0.7			
C_3A	0.3	2.64×10^{-10}		
	0.5			
	0.7			
C_3AF	0.3	0.42×10^{-10}		
	0.5	2.64×10^{-10}		
	0.7	15.6×10^{-10}		

References

[1] J. Piasta, Heat deformations of cement paste phases and the microstructure of cement paste, Materiaux et Constructions 17 (102) (1984) 415–420.
[2] U. Schneider, H. Herbst, Permeability and porosity of concrete at high temperature, Technical report 403, Deutscher Ausschuss für Stahlbeton, Berlin, In German, 1989.
[3] J. Piasta, Z. Sawicz, L. Rudzinski, Changes in the structure of hardened cement paste due to high temperature, Materiaux et Constructions 17 (100) (1984) 291–296.
[4] W.M. Lin, T.D. Lina, L.J. Powers-Couche, Microstructures of fire-damaged concrete, ACI Materials Journal 93 (3) (1996) 199–205.
[5] X.S. Wang, B.S. Wu, Q.Y. Wang, Online SEM investigation of microcrack characteristics of concretes at various temperatures, Cement and Concrete Research 35 (7) (2004) 1385–1390.
[6] G. Constantinides, F.J. Ulm, The effect of two types of C-S-H on the elasticity of cement-based materials: results from nanoindentation and micromechanical modeling, Cement and Concrete Research 34 (11) (2004) 1293–1309.
[7] O. Bernard, F.J. Ulm, E. Lemarchand, A multiscale micromechanics-hydration model for the early-age elastic properties of cement-based materials, Cement and Concrete Research 33 (9) (2003) 1293–1309.
[8] D.P. Benz, Influence of water-to-cement ratio on hydration kinetics: Simple models based on spatial considerations, Cement and Concrete Research 36 (2) (2006) 238–244.
[9] H.F.W. Taylor, Cement Chemistry, Academic Press, New York, 1997.
[10] T.C. Hansen, Physical structure of hardened cement paste. A classical approach, Material and Structures 19 (114) (1986) 423–436.
[11] Z. Bazant, M. Kaplan, Concrete at High Temperatures, Material Properties, and Mathematical Models, Longman, Burnt Mill, UK, 1996.
[12] L.E. Copeland, R.H. Bragg, The determination of non-evaporable water in hardened Portland cement paste, ASTM Bulletin, vol. 194, ASTM, Philadelphia, 1953, pp. 70–74.
[13] P.D. Tennis, H.M. Jennings, A model for two types of calcium silicate hydrate in the microstructure of Portland cement pastes, Cement and Concrete Research 30 (6) (2000) 855–863.
[14] T.Z. Harmathy, Thermal properties of concrete at elevated temperature, ASTM Journal of Materials 5 (1) (March 1970) 47–74.
[15] T.C. Powers, Physical properties of hardened cement paste, Proceeding of the Fourth International Symposium on the Chemistry of Cement, 22, Washington DC, 1960, pp. 577–609.
[16] Y. Xi, A Composite Theory for Diffusivity of Distressed Materials, Proc. of 15th ASCE Engineering Mechanics Conference, Columbia University, New York, June 2–6 2002, available on CD-ROM and online (http://www.civil.columbia.edu/em2002/, paper No. 535).
[17] Y. Xi, A. Nakhi, Composite damage models for diffusivity of distressed materials, Journal of Materials in Civil Engineering, ASCE 17 (3) (May/June 2005) 286–295.
[18] Y. Xi, M. Eskandari-Ghadi, Suwito, S. Sture, A damage theory based on composite mechanics, Journal of Engineering Mechanics, ASCE 132 (11) (2006) 1–10.
[19] P. Acker, Micromechanical analysis of creep and shrinkage mechanisms, creep, shrinkage and durability mechanics of concrete and other quasi-brittle materials, Proc. of the Sixth International Conference CONCREEP6, Elsevier, Oxford, UK, 2001, pp. 15–25.
[20] K. Velez, S. Maximilien, D. Damidot, G. Fantozzi, F. Sorrentino, Determination by nanoindentation of elastic modulus and hardness of pure constituents of Portland cement clinker, Cement and Concrete Research 31 (4) (2001) 555–561.
[21] J.J. Beaudoin, Comparison of mechanical properties of compacted calcium hydroxide and Portland cement paste systems, Cement and Concrete Research 13 (3) (1983) 319–324.
[22] F.H. Wittmann, Estimation of the modulus of elasticity of calcium hydroxide, Cement and Concrete Research 16 (6) (1986) 971–972.
[23] P.J.M. Monteiro, C.T. Chang, The elastic moduli of calcium hydroxide, Cement and Concrete Research 25 (8) (1995) 1605–1609.
[24] H. Oda, O.L. Anderson, D.G. Isaak, I. Suzuki, Measurement of elastic properties of single-crystal CaO up to 1200 K, Physics and Chemistry of Materials 19 (1992) 96–105.
[25] J.S. Lee, Y. Xi, K. Willam, Concrete after high temperature heating and cooling, ACI Materials Journal 105 (4) (2008) 334–341.
[26] R. Berliner, M. Popovici, K.W. Herwig, M. Berliner, H.M. Jennings, J.J. Thomas, Quasielastic neutron scattering study of the effect of water-to-cement ratio on the hydration kinetics of tricalcium silicate, Cement and Concrete Research 28 (2) (1998) 231–243.
[27] H.F.W. Taylor, A method for predicting alkali ion concentration in cement pore solutions, Advances in Cement Research 1 (1) (1987) 5.
[28] K. Fuji, W. Kondo, Kinetics of the hydration of tricalcium silicate, Journal of the American Ceramic Society 57 (1974) 492–502.